Biophysical Chemistry 160 (2012) 20–27

Contents lists available at SciVerse ScienceDirect

Biophysical Chemistry

journal homepage: http://www.elsevier.com/locate/biophyschem

Effect of charged lidocaine on static and dynamic properties of model bio-membranes

Zheng Yi [a], Michihiro Nagao [b,c], Dobrin P. Bossev [c,*]

[a] UT/ORNL Center for Molecular Biophysics, Oak Ridge National Laboratory, Oak Ridge, TN 37831, United States
[b] Center for Neutron Research, National Institute of Standards and Technology, Gaithersburg, MD 20899, United States
[c] Center for Exploration of Energy and Matter, Indiana University, Bloomington, IN 47408, United States

HIGHLIGHTS

- We investigated the effect of lidocaine on DMPC membranes.
- Lidocaine in membrane causes lateral expansion and decreases thickness.
- Change in the membrane structure induces depression of the tail group ordering.
- Lidocaine increases the bending elasticity of DMPC membranes.

GRAPHICAL ABSTRACT

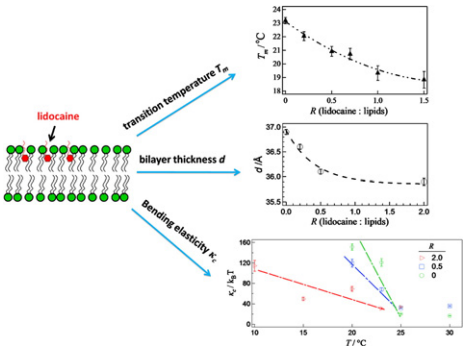

ARTICLE INFO

Article history:
Received 22 July 2011
Received in revised form 28 August 2011
Accepted 30 August 2011
Available online 10 September 2011

Keywords:
Lidocaine
Phospholipid
Membrane
Neutron spin echo
Bending elasticity

ABSTRACT

The effect of the charged lidocaine on the structure and dynamics of DMPC/DMPG (mass fraction of 95/5) unilamellar vesicles has been investigated. Changes in membrane organization caused by the presence of lidocaine were detected through small angle neutron scattering experiments. Our results suggest that the presence of lidocaine in the vicinity of the headgroups of lipid membranes leads to an increase of the area per lipid molecule and to a decrease of membrane thickness. Such changes in membrane structure may induce disordering of the tail group. This scenario explains the reduction of the main transition temperature of lipid membranes, as the fraction of lidocaine per lipid molecules increases, which was evident from differential scanning calorimetry results. Furthermore neutron spin echo spectroscopy was used for the dynamics measurements and the results reveal that presence of charged lidocaine increases the bending elasticity of the lipid membranes in the fluid phase and slows the temperature-dependent change of bending elasticity across the main transition temperature.

1. Introduction

Artificially synthesized lipid bilayers have been widely used as model systems for elucidation of basic processes occurring in biological membranes as well as for certain biotechnological applications [1–7]. In pharmaceutical research, several commercial and scientific applications of lipid bilayers to form drug containing vesicles have found potential applications as drug delivering vehicles [8]. Lipid vesicles also have been served as the models for investigating the interactions between membranes and drugs [9–11]. A variety of methods have been used on artificial lipid membranes and demonstrated that the membrane properties may be strongly affected by the presence of membrane-associated molecules. The conformation of acyl groups, the membrane density, and thickness as well as membrane dynamics are examples of parameters that can be affected by drug–membrane interactions [12–14]. In this study small angle neutron scattering (SANS) and neutron spin-echo (NSE) spectroscopy have been used to shed light on

* Corresponding author at: Physics Department, Indiana University, Bloomington, IN 47405, United States. Tel.: +1 812 855 9407; fax: +1 812 855 6645.
E-mail address: dbossev@indiana.edu (D.P. Bossev).

0301-4622/$ – see front matter © 2011 Elsevier B.V. All rights reserved.
doi:10.1016/j.bpc.2011.08.007

the effect of charged lidocaine, one of the most widely used local anesthetics (LA) [15], on the static and dynamic properties of artificial lipid membranes.

LAs are known to produce loss of sensation to pain in the certain area of the body without the loss of consciousness [16]. Despite the fact that LAs have been clinically used for more than a century, a detailed description of LA mechanisms of action is still an open debate. In recent decades the most prevailing hypothesis of the anesthetic action is that LA directly binds the specific sites in transmembrane proteins which work as voltage-gated Na^+ channels in nerve membranes thus reduces the influx of sodium ions into the nerve cytoplasm and finally results in the inhibition of the depolarization of the nerve [17–21]. However, the lipid bilayers function not just as medium to host and support protein machinery, the composition of the membrane is sometimes indispensible for many protein functions. Many researches are focused on the interaction of anesthetic molecules with the lipid phase of the membranes [14,22–25]. A number of papers reported that LA also interact with the lipid membranes and alter their organizational properties. Such changes in the biological membranes may interfere with lipid–protein interactions leading to protein conformational changes with consequences to their activity.

Previous NMR experiments have confirmed that the polar parts of LA interact with phospholipid polar fragments and their lipophilic parts insert in the bilayer hydrophobic region [26–28]. The intercalation which is also called hydrophobic mismatch between the bio-membranes and LA can induce configurational disorder of membranes which may also influence some physical and mechanical parameters of the bio-membranes. First of all, many synthetic membranes made of phospholipids undergo a first-order acyl-chain melting transition which is called main transition from the ripple gel ($P_{\beta'}$) to the fluid (L_α) phases. Hata et al. have already examined that the main transition temperature (T_m) of 1,2-dipalmitoyl-*sn*-glycero-3-phosphocholine (DPPC) bilayers is depressed by several LA types: dibucaine, tetracaine, bupivacaine, lidocaine and procaine [23]. In the present study charged lidocaine is focused on investigating the effect of LA on the phase behavior of DMPC/DMPG unilamellar vesicles (ULV). DMPC (1,2-dimyristoyl-*sn*-glycero-3-phosphocholine) is one of the most extensively studied ester-linked phospholipids with regard to its structural and thermodynamic properties [29–31]. ULVs formed from a mixture of DMPC (zwitterionic lipid with bulkier headgroup) and small amount of DMPG (1,2-dimyristoyl-*sn*-glycero-3-phosphoglycerol, anionic lipid with relatively smaller headgroup) substantially improve the stability and degree of alignment compared with ULVs formed by a single type of lipid [32–33]. The bilayer thickness (d) of bio-membranes, defined as the distance between headgroups of the both sides of the bilayer, has been identified as an important factor in the insertion, folding, multimeric assembly and function of transmembrane proteins [34–35]. We have attempted to clarify how the influence of lidocaine on bilayer thickness can help us in understanding the possibility that drugs indirectly alter membrane protein functions by changing the structure of lipid bilayer, thereby changing the local environment of membrane proteins. To answer this question we have used SANS to investigate the influence of lidocaine on the bilayer thickness in aqueous solutions of synthesized DMPC/DMPG ULVs. Further we have focused on the bending elasticity (κ_c) of bio-membranes as an important mechanical property that governs the thermal fluctuation of bilayers, which in turn gives rise to undulation forces and predetermines the contact time of the membranes with solid substrates and other objects [36].

In this study we have attempted to elucidate the influence of LA on the bending elasticity of model phospholipid membranes. We have chosen neutron-spin-echo (NSE) spectroscopy as the most suitable method to determine κ_c. NSE is a dynamic method ideal for studies of the thermal fluctuations of the bio-membranes because of its correlation times (0.1 ns to 100 ns) and length scales (10 Å to 10^3 Å) that are characteristic for the cell membrane fluctuations [37–38]. In this paper the bending elasticities of DMPC ULV bilayers with different concentrations of lidocaine above and below T_m were measured by NSE. The intermediate scattering function acquired through NSE was explained by the Zilman–Granek model [39–40] for 2-D membranes. What needs to be mentioned is that because of the at-detector neutron flux limitations originating principally from the nature of the primary neutron source, medically irrelevant high molar ratio of lidocaine was used in this research to enhance the effect of charged lidocaine on membranes.

2. Materials and methods

2.1. Materials

Synthetic 1,2-dimyristoyl-*sn*-glycero-3-phosphocholine (DMPC) and 1,2-dimyristoyl-*sn*-glycero-3-phospho-*rac*-(1-glycerol) (DMPG) were purchased from Avanti® Polar Lipids (Alabaster, AL) and used without further purification. The 2-diethylamino-N-(2,6-dimethylphenyl) acetamide (charged lidocaine) hydrochloride monohydrate was purchased from Sigma Chemicals (St. Louis, MO) in the solid form. Deuterated water, D_2O, (99% atomic percent) was purchased from Cambridge Isotope Labs, (Andover, MA). These materials were used without further purification.

2.2. Sample preparation

DMPC/DMPG bilayers of unilamellar vesicles were prepared by the extrusion method [41]. Mass fractions of 95% DMPC and 5% DMPG were mixed together with a certain weight percentage of lidocaine (molar ratio R between lidocaine and lipids = 0, 0.2, 0.5, 0.7, 1.0, and 2.0). DMPG is an anionic lipid and structurally similar to DMPC but is negatively charged because of the presence of PO_4 group and a lack of the positive charge of the choline group. The presence of small amount of DMPG has been proven to enhance the electrostatic repulsion between the lipid bilayers which can stabilize the states of the vesicles [32]. The mixed DMPC/DMPG/lidocaine was dissolved in high performance liquid chromatography (HPLC) grade chloroform to ensure good mixing. After that the organic solvent was evaporated under the nitrogen gas for no less than 3 h. The remaining thin films of lipids were then placed in a vacuum chamber at 60 °C for over 6 h to evaporate the solvent residuals. The necessary amount of D_2O was added to get a lipid concentration of a mass fraction of 1.0% for SANS and 2.0% for NSE. At these concentrations the distance between different vesicles is large enough to neglect the inter-vesicle interactions [32]. For the DSC measurement mixture of a mass fraction of 10% lipid in D_2O was prepared. The uniform dispersion was obtained by repetitive freezing down to −10 °C, heating above the main phase transition temperatures and vortexing. Finally ULVs were prepared by an Avanti Mini-Extruder for SANS and NSE measurements. The dispersion was extruded through a polycarbonate filter from Whatman Inc. (Florham Park, NJ) with pore diameter of 1000 Å. About 30 passes were performed to minimize the contamination of the sample by multilamellar vesicles (MLVs) and give rise to the diameter of the vesicles smaller than the filter pore size.

2.3. Dynamic light scattering (DLS)

The average sizes of the vesicles at 30 °C were characterized by dynamic light scattering (DLS). The extruded samples for SANS and NSE were diluted with adding D_2O in order to get a mass fraction of 0.1% lipid vesicle solutions, so that we can evaluate the mean diffusion constant from our DLS measurements. With a DynaPro-Titan DLS system that uses a He–Ne ion laser ($\lambda = 783$ nm) as a light source we determined the normalized intensity time correlation function. Through the inverse Laplace transform analysis one can obtain the relaxation time distribution. From the moments of this distribution the mean

diffusion coefficients of the particles, D, were determined [25]. The hydrodynamic radius of vesicles R_H was then obtained using the Stokes–Einstein equation:

$$R_H = \frac{kT}{6\pi\eta_0 D}, \quad (1)$$

where k is the Boltzman constant, T is the absolute temperature, and η_0 is the solvent viscosity.

2.4. Differential scanning calorimetry (DSC)

Differential scanning calorimetry (DSC) was used to investigate the effect of charged lidocaine on the main transition temperatures T_m of DMPC/DMPG membranes. The thermotropic phase behaviors of MLVs of $R = 0$, 0.2, 0.5, 0.7, 1.0 and 1.5 (a mass fraction of lipids in D_2O of 10%) were determined by TA instruments Q1000 differential scanning calorimeter (New Castle, DE). The temperature scanning was from 30 °C to 0 °C and reverse back to 30 °C with the temperature accuracy of ±0.1 °C. The heating and cooling scanning rates were 1 °C per minute.

2.5. Small angle neutron scattering (SANS)

SANS measurements were performed at the NG3-30 m SANS instrument at National Institute of Standards and Technology (Gaithersburg, MD) [42]. Neutrons of wavelength $\lambda = 8.4$ Å with a wavelength spread of $\Delta\lambda/\lambda = 11\%$ were used in our experiment. Data were collected with a two-dimensional detector at three different sample-to-detector distances (1.3 m, 4.0 m, and 13.7 m) in order to span the range of scattering vectors q from 2×10^{-3} Å^{-1} to 4×10^{-1} Å^{-1}, where $q = 4\pi \sin(\theta/2)/\lambda$, and θ is the scattering angle. Samples were contained in 1 mm path-length quartz cells. The data were corrected for instrumental and empty cell backgrounds using the Igor Pro based reduction macros supplied by NIST [43]. Samples of $R = 0$, 0.2, 0.5, 0.7, 1.0, and 2.0 were measured at 30 °C in L_α phase, which is above T_m of DMPC/DMPG mixtures [44–45]. The temperature was controlled by water circulation bath with an accuracy of ±0.1 °C.

2.6. Neutron spin echo spectroscopy (NSE)

The NSE technique has been widely used in the study of dynamic processes in macromolecular systems that are relevant to, among others, polymer and biomedical sciences [46–48]. The NSE spectrometer measures the real part of the intermediate scattering function, $I(q,t)$ in the time domain. Our data were taken on the spectrometer located at the NG5 guide of the NIST Center for Neutron Research (NCNR) [49]. Neutrons with wavelengths of either 8.0 Å or 11.6 Å were used to cover q ranges from 0.03 Å^{-1} to 0.12 Å^{-1} and time t from 0.1 ns to 90 ns. The collected NSE data were reduced in terms of the experimental background and resolution using the NCNR program DAVE [50]. The temperature dependence of the bending elasticity was measured for samples with $R = 0$, 0.5, and 2.0 at several temperatures from 10 °C to 30 °C.

3. Results

Representative high-sensitivity DSC scans for DMPC/DMPG bilayers are presented in Fig. 1(a). It is well known that in the absence of foreign solutes, many phospholipid bilayer membranes exhibit two endotherms on heating, a lower temperature, lower enthalpy pretransition and a higher temperature, higher enthalpy main transition. The pretransition arises from the conversion of the lamellar gel ($L_{\beta'}$) phase to $P_{\beta'}$ phase, and the main transition from a conversion of the $P_{\beta'}$ phase to L_α phase. In Fig. 1(a), the main transition temperature T_m from $P_{\beta'}$ to L_α phase of pure DMPC/DMPG bilayers was observed at 23.2 °C, which is in good agreement with previously published data [51–52]. However due to the rapid heating/cooling scanning rate (1 °C/min), the pretransition temperature T_p of the bilayers wasn't monitored [53]. A bimodal endothermic transition peak of the main transition was observed in all samples that contain lidocaine and became more depressed and broader as R increased. The appearance of this bimodal melting peak, instead of single transition peak, probably indicates a relatively broad distribution of lidocaine/lipids ratio in the solution. In order to illustrate the effect of the charged lidocaine on T_m, R dependence of T_m is presented in Fig. 1(b). It clearly shows that the addition of charged lidocaine progressively depresses T_m. The characteristic shift in T_m is probably due to the increasing disorder of the hydrophobic core of DMPC/DMPG bilayers caused by the presence of the charged lidocaine. This will be further addressed in the Discussion section.

The reduced SANS intensities as a function of q at 30 °C are shown in Fig. 2. The macroscopic phase state of the samples was visually inspected before each measurement to ensure homogeneity of the samples. The solutions of $R = 0$, 0.2, 0.5, and 2 were homogenous during the measurement, suggesting the stability of their unilamellar phases. Clear phase separations were observed in the samples of $R = 0.7$ and 1. The multilamellar peaks in Fig. 2 at $q \approx 0.1$ Å^{-1}, together with the broad distribution of the vesicle sizes in DLS measurement (data not shown) indicate the existence of MLVs in these two samples. MLVs have excess water in the system comparing with unilamellar ones, therefore the mixture of MLVs and ULVs may lead to the macroscopic phase separation. The appearance of the multilamellar phase probably correlates with the saturation ratio of membranes and foreign solutes [54–55].

For the analysis of the structural change during the increase of lidocaine concentration, the measured scattering intensities of DMPC/

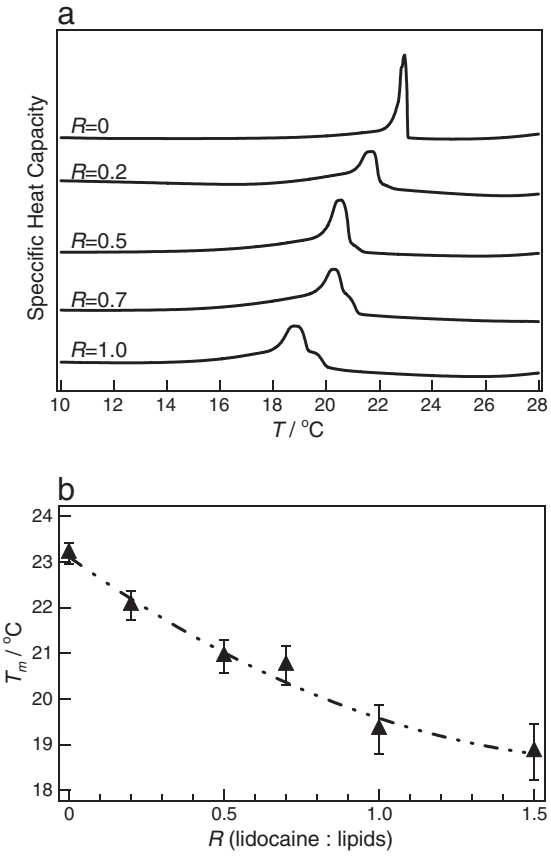

Fig. 1. (a) Differential scanning calorimetry (DSC) thermogram of DMPC/DMPG bilayers with different molecular ratios R. (b) Representative plot of the main transition temperature T_m of DMPC/DMPG bilayers in D_2O as a function of R. T_m was empirically fitted as a function of R^2.

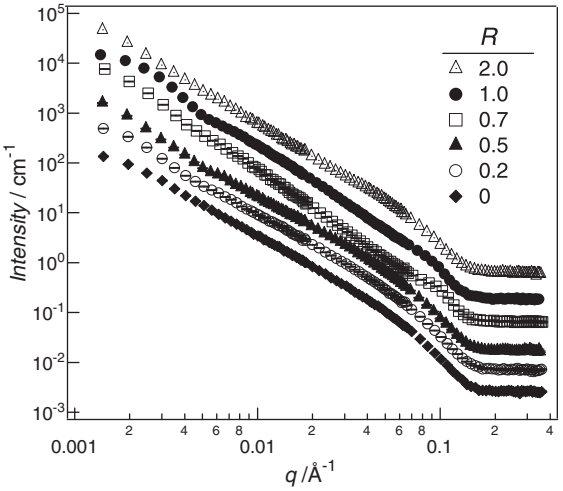

Fig. 2. SANS curves for samples of $R=0$, 0.2, 0.5, 0.7, 1.0, and 2.0 (from bottom to top) at 30 °C as a function of q. Curves were vertically shifted for better readability. Error bars represent ±one standard deviation throughout the paper.

DMPG ULV bilayers are fitted to a model of polydispersed spherical shells (PSS) [32,43,56] whose intensity can be expressed as:

$$I(q)=\int_r G(r)P(q,r)dr=\int_r G(r)\left[4\pi\int_{r_1}^{r_2} r^2\rho(r)\frac{\sin(qr)}{qr}dr\right]^2 dr, \tag{2}$$

where $\rho(r)$ is the scattering length density (SLD) as a function of radial distance from the center of the vesicle, r is the distance between the center of the vesicle and that of the bilayer, d is the bilayer thickness and $r_1=r-d/2$ and $r_2=r+d/2$. If the SLD of vesicles is treated as constant across the bilayers, the form factor $P(q,r)$, as determined via Born Approximation [57], is given by:

$$P(q,r)=(\rho-\rho_0)^2\left[r_2{}^3\frac{j_1(qr_2)}{qr_2}-r_1{}^3\frac{j_1(qr_1)}{qr_1}\right]^2, \tag{3}$$

where ρ is the averaged SLD of the membrane, ρ_0 is the SLD of D_2O, and $j_1(x)$ is the first-order spherical Bessel function:

$$j_1(x)=\frac{\sin x-x\cos x}{x^2}. \tag{4}$$

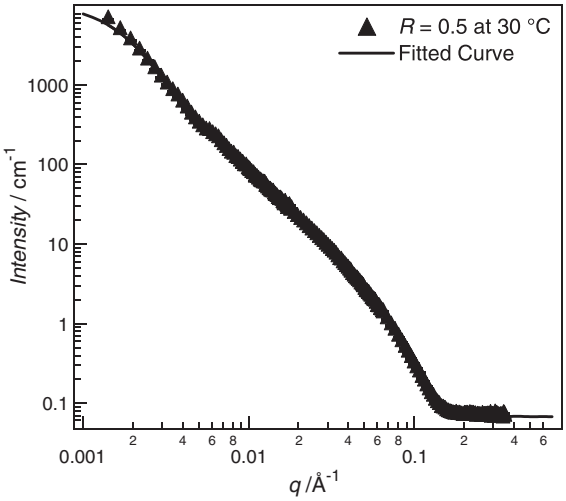

Fig. 3. SANS spectrum of the DMPC/DMPG vesicle of $R=0.5$ at 30 °C (triangles) and fitted curve (solid line) with the assumption of $\rho(r)=$constant.

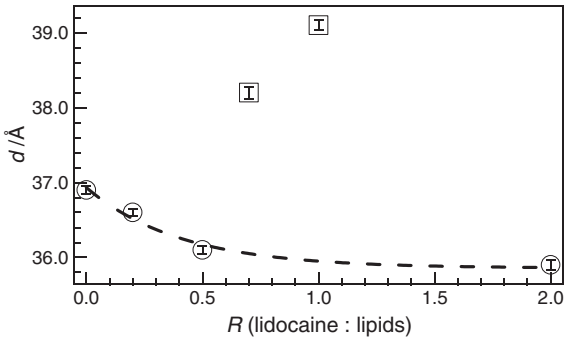

Fig. 4. The plot of bilayer thickness d as the function of R. d was empirically fitted with an exponential function of R. The larger d of the samples of $R=0.7$ and 1.0 is due to the co-existence of MLVs and ULVs.

In order to take into account the influence of vesicle size polydispersity, the size distribution function $G(r)$ is assumed as the Schulz distribution [58]:

$$G(r)=\left(\frac{z+1}{r_m}\right)^{z+1}\frac{r^z}{\Gamma(z+1)}\exp\left[\frac{-r(z+1)}{r_m}\right], \tag{5}$$

where r_m is the mean radius. The variance and the polydispersity (relative variance) are calculated as $\sigma^2=r_m^2/(z+1)$ and $\Delta^2=1/(z+1)$, respectively.

The representative fit of the sample of $R=0.5$ is shown in Fig. 3. Note that during the data analysis the SLD profile in our model consists of one homogenous strip whereas the SLD difference, $\rho-\rho_0$, is taken as constant through the bilayer with sharp interfaces. Our calculated bilayer thickness for pure unilamellar DMPC/DMPG bilayers $d=(36.9\pm0.05)$ Å is comparable to the results of Kucerka et al. [7] obtained from SAXS data with DMPC steric bilayer thickness $d_{HH}=35.3$ Å and that of Lewis and Engelman [59] whose calculated phosphate peak spacing of DMPC is $d=(34\pm1)$ Å. The calculated bilayer thickness d of the lipids/lidocaine mixtures is plotted as a function of R in Fig. 4. The PSS model successfully fit the samples of $R=0$, 0.2, 0.5, and 2.0, and their bilayer thicknesses d decrease exponentially with increasing R, similar to previous studies [60]. For the solutions of $R=0.7$ and 1.0, because of the co-existence of MLVs and ULVs in the system, the bilayer thickness d obtained from the PSS model is slightly larger than that of other solutions. Therefore, we omit the data points for $R=0.7$ and 1.0 in the following parts of the paper.

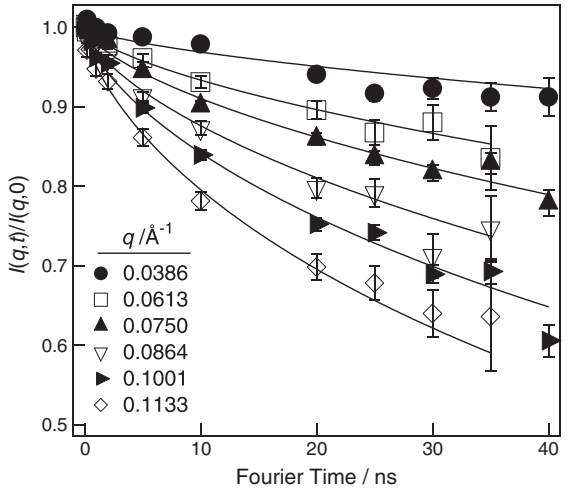

Fig. 5. The intermediate scattering functions $I(q,t)$ normalized to $I(q,0)$ obtained by NSE against Fourier time t at different q values for DMPC/DMPG ULVs with $R=0$ in D_2O at 25 °C.

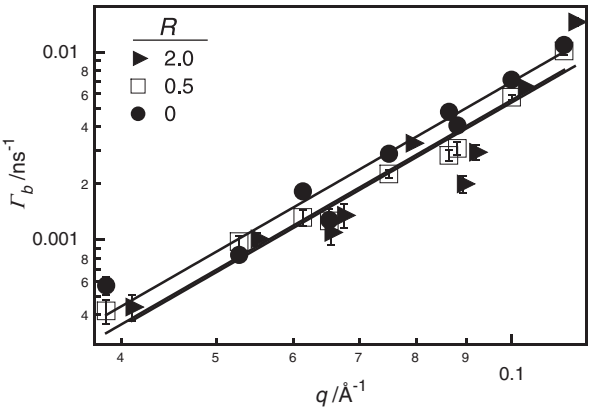

Fig. 6. Relaxation rate Γ for DMPC/DMPG ULV bilayers with $R=0$, 0.5, and 2.0 in D_2O at 25 °C as a function of the scattering vector q. The solid lines are fits to Eq. 8.

Bio-membranes in aqueous solution exhibit thermal undulations which are strongly dependent on the mechanical properties of bilayers such as the bending elasticity. The thermal undulations of phospholipid bilayers have been successfully probed by NSE and the membrane dynamics in the lamellar phase are qualitatively explained by the theory given by Zilman and Granek [39–40]. If the system forms vesicles, shape fluctuations of the vesicles should be observed similarly to microemulsion systems [61]. However the length scale we are probing is intermediate to the membrane thickness and the radius of the vesicles. The shape fluctuations of the vesicles are observed at the q range corresponding to the radius of the vesicles, characterized by the dip position in the small-angle scattering curve (in the present case we saw a dip around $q=0.003$ Å^{-1}, which is far below the low q limit accessible by our NSE). Therefore in the measured q-range the scattering originated not from the entire vesicle as a whole but from a fraction of it. In this case the isolated single membrane fluctuation model is suitable.

The NSE directly measures the intermediate scattering function $I(q,t)$, which is a cosine Fourier transform of the dynamic structure factor $S(q,\omega)$:

$$I(q,t)=\int_{-\infty}^{+\infty} S(q,\omega)\cos(\omega t)d\omega, \tag{6}$$

where t is the time, ω is the energy transfer for the scattered neutrons and $S(q,\omega)$ is a function that uniquely reflects the scattering probabilities of the sample. The time decay of $I(q,t)$ originating from thermal undulations of isolated single membranes is predicted to exhibit stretched exponential decay [39–40]:

$$I(q,t)=I(q,0)e^{-(\Gamma_b t)^{2/3}}, \tag{7}$$

where Γ_b is the relaxation rate, and related to the bending elasticity as:

$$\Gamma_b=0.025\gamma_k\left(\frac{k_BT}{\kappa_c}\right)^{\frac{1}{2}}\frac{k_BT}{\eta}q^3, \tag{8}$$

Table 1
Bending elasticity κ_c/K_BT of DMPC/DMPG bilayers in the presence of charged lidocaine with different R in D_2O. The values are calculated from Eq. 8 at different temperatures.

T/°C	$R=0$	$R=0.5$	$R=2.0$
10	–	–	114.4 ± 10.5
15	–	–	49.8 ± 3.5
20	151.0 ± 6.1	119.5 ± 7.7	69.4 ± 4.7
23	120.7 ± 7.4	68.2 ± 3.3	31.0 ± 1.4
25	20.4 ± 0.7	31.8 ± 1.2	33.8 ± 1.5
30	16.7 ± 0.5	35.9 ± 1.2	–

where η is the solvent viscosity and the factor γ_k originates from averaging over the angle between the wave vector and the plaquette surface normal in the calculation of $I(q,t)/I(q,0)$. The parameter γ_k approaches unity when $\kappa_c \gg k_BT$. We use three times the value of average solvent ($\eta=3\eta_{solvent}$) for viscosity η when taking the local dissipation at the membrane into consideration [37,62–64]. Fig. 5 shows $I(q,t)/I(q,0)$ obtained by NSE at different q values from (0.05 to 0.12) Å^{-1} for pure DMPC/DMPG vesicles of $R=0$ at 25 °C. The solid lines were fits to Eq. 7. The fits confirmed that the NSE decay reflects predominantly the thermal fluctuations exhibited by the lipid bilayers.

The calculated relaxation rate Γ_b as a function of q in a double logarithmic plot of DMPC/DMPG ULV bilayers with $R=0$, 0.5 and 2.0 in D_2O at 25 °C is shown in Fig. 6 where the solid lines are fits to Eq. 8. When fitted by a power law with a variable exponential factor we have found the slope to vary within 2.6 to 3.4 which is close to 3 as predicted by Eq. 8. The good fitting verifies the q^3 dependence of the relaxation rate Γ_b and indicates that the NSE result directly shows the relaxation of the membrane undulation. Hence Eq. 8 can be safely used to calculate the bending elasticity. The numerical data κ_c of DMPC/DMPG bilayers with $R=0$, 0.5, and 2.0 in D_2O are tabulated in Table 1 and shown in Fig. 7. The presence of charged lidocaine results in three effects, the shift of T_m, increase of κ_c in L_α phase, and the slowing of the L_α to $P_{\beta'}$ transition, which will be discussed in details in Discussion.

4. Discussion

Our DSC and SANS measurements show that the presence of charged lidocaine depresses T_m of DMPC/DMPG bilayers, broadens their endothermic peaks, and causes the thickness reduction. These changes in thermodynamics and structures of the lipid bilayers induced by local anesthetics are quite similar to the effect of general anesthetics on biomembranes, but different from the influence by the presence of cholesterol. Here we try to discuss these results all together and have a more general explanation for the foreign molecule–lipid interactions.

Similarly to lidocaine, both general anesthetics, such as halothane, and cholesterol are weakly amphiphilic substances. However cholesterol is more hydrophobic and has low solubility in water. McMullen et al. [53] performed DSC scans of DPPC bilayers with various cholesterol molar concentrations and confirmed that the addition of cholesterol broadens T_m and when cholesterol fraction is above $R=0.5$ the endothermic peak of main phase transition completely disappears. Cholesterol inserts into bilayers perpendicular to the membrane plane with its hydroxyl group oriented toward the aqueous phase and its hydrophobic ring system adjacent to hydrocarbon tails of phospholipids. The presence of those rigid cholesterol molecules disrupts the normal reactions between hydrocarbon chains of phospholipids, and results in membranes that are less fluid and less subject to phase transitions. The effect of cholesterol on T_m was attributed to the mismatch between the effective hydrophobic length of the cholesterol molecule and the

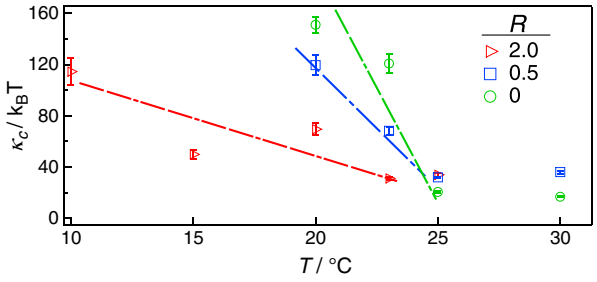

Fig. 7. The bending elasticity κ_c of DMPC/DMPG bilayer with lidocaine concentration of $R=0$, 0.5 and 2.0 in D_2O plotted against T. The presence of charged lidocaine results in the shift of T_m, increase of κ_c in L_α phase, and the broadening of the L_α to $P_{\beta'}$ transition.

hydrocarbon core of the host phosphotidylcholine bilayers [65–66]. Furthermore, the presence of cholesterol causes the phospholipid acyl chains close to the headgroup to have predominantly a trans configuration, leading to an increase in bilayer thickness and an increase in polar region hydration [65,67–71].

Different from cholesterol, the lidocaine molecules are positioned in the membrane–water interface and may compete for water molecules with lipid headgroups [72–73]. The charged lidocaine molecules were located close to the polar headgroup of the lipids. This finding accords with the results of general anesthetics from both experiments and MD simulations [74–77], showing that general anesthetics partitions near the lipid–water interface close the lipid glycerol backbone and upper segments of lipid hydrocarbon chains. The insertion of the charged lidocaine and general anesthetics in the lipid headgroups provide more inter-molecular spacing between lipids. The increased inter-molecular spacing provides more volume accessible to lipid molecules and higher disordering between their hydrocarbon chains [78], and finally results in the lowering of the gel-to-fluid phase transition temperatures.

In our previous paper [31] the effect of temperature on bending elasticity κ_c of pure lipid ULVs in D_2O was examined. We have found that at $T \gg T_m$, κ_c of pure DMPC/DMPG bilayers is independent of temperature hence the temperature has a minimal effect on the properties of the lipid bilayer in L_α phase. When the temperature is approaching the main transition temperature, κ_c becomes slightly larger [30]. A strong decrease of κ_c was observed when T reaches T_m by other experimental methods [79–81], i.e. optical dynamometry. The decrease is more pronounced with multilamellar membranes, and was attributed to a drop in the area compressibility modulus K_A [80–81]. This behavior relates to the so-called anomalous swelling. The origin of the increase in κ_c around T_m has been systematically investigated by Seto et al. [30], while it is out of the scope of our discussion, and thus we would not discuss further here. At $T<T_m$, the system is in the $P_{\beta'}$ phase and κ_c rapidly increases 6–10 times compared with that in L_α phase. We find that the results of DMPC/DMPG bilayers with different R also obey the above trend with some specific characteristics as shown in Fig. 7.

Through the NSE measurements, three effects of lidocaine on the bending elasticity of lipid bilayers have been found. First, in the vicinity of T_m of DMPC/DMPG bilayers (at 25 °C and 30 °C) κ_c increases from 16.7 k_BT for $R=0$ to 33.8 k_BT for $R=2.0$. Our previous research has proven that the bending elasticity should scale as the area compressibility modulus K_A multiplied by the square of the hydrophobic thickness d^2[31,79,82–83]:

$$\kappa_c = \beta K_A d^2 \tag{9}$$

where β is a normalization constant. Since the bilayer thickness decreases with the presence of charged lidocaine, the increase of κ_c can be attributed to the increase of the area modulus K_A of DMPC/DMPG ULVs in L_α phase. Second, the results of NSE also confirmed that T_m is decreased in the presence of lidocaine. T_m locates between 23 °C and 25 °C for the sample of $R=0$, and then left shifts between 20 °C and 23 °C for the sample of $R=2$. Third, the bending elasticities at different R change with different trends in a lidocaine-dose-dependent manner. The straight lines in Fig. 7 show the trend. The values of κ_c at $R=0$ have the steepest increase from L_α to $P_{\beta'}$ phase whereas that at $R=2.0$ increases the slowest, indicating the incremental disordering of the bilayers and reduced membrane stiffness at $T<T_m$ caused by charged lidocaine.

5. Conclusions

We have used DLS, DSC, SANS and NSE to probe the influence of lidocaine on the structural and dynamic properties of DMPC/DMPG bilayers. Our results confirmed that the lidocaine molecules loosen the packing of the membrane constituent lipids and induce lateral membrane expansion. The intercalation of lidocaine molecules provides more inter-molecular space between the lipid molecules and results in the decrease of the bilayer thickness. It is also found that the presence of charged lidocaine doubles κ_c in the L_α phase, while slows the increase of κ_c when T decrease from $P_{\beta'}$ to L_α phase. The presence of charged lidocaine enlarges the area modulus K_A of DMPC/DMPG bilayers that overcomes the effect of thinning of the membrane to increase κ_c.

Acknowledgments

The authors acknowledge Tatiana Psurek for her help to our DSC measurements. This work utilized facilities supported in part by the National Science Foundation under Agreement No. DMR-944772. We acknowledge the support of the National Institute of Standards and Technology, U.S. Department of Commerce, in providing the neutron research facilities used in this work. We thank Antonio Faraone for his valuable discussion and his help with the data collection at NCNR and Larry Kneller for his support in our data analysis.

Certain trade names and company products are identified in order to specify adequately the experimental procedure. In no case does such identification imply recommendation or endorsement by the National Institute of Standards and Technology, nor does it imply that the products are necessarily the best for the purpose.

References

[1] L.T. Mimms, G. Zampighi, Y. Nozaki, C. Tanford, J.A. Reynolds, Phospholipid vesicle formation and transmembrane protein incorporation using octyl glucoside, Biochemistry 20 (1981) 833–840.
[2] C. Sebban, Y. Lasne, V. Berenguer, E. Archimbaud, Y. Devaux, J.J. Viala, CA125 and malignant lymphomas, Journal of Clinical Oncology 9 (1991) 359–360.
[3] C.S. Vassilieff, I. Panaiotov, E.D. Manev, J.E. Proust, T. Ivanova, Kinetics of liposome disintegration from foam film studies: effect of the lipid bilayer phase state, Biophysical Chemistry 58 (1996) 97–107.
[4] F.J. Sharom, The P-glycoprotein multidrug transporter: interactions with membrane lipids, and their modulation of activity, Biochemical Society Transactions 25 (1997) 1088–1096.
[5] C. Honninger, F. Morier-Genoud, M. Moser, U. Keller, L.R. Brovelli, C. Harder, Efficient and tunable diode-pumped femtosecond Yb:glass lasers, Optics Letters 23 (1998) 126–128.
[6] S.L. Veatch, S.L. Keller, Separation of liquid phases in giant vesicles of ternary mixtures of phospholipids and cholesterol, Biophysical Journal 85 (2003) 3074–3083.
[7] N. Kucerka, Y. Liu, N. Chu, H.I. Petrache, S. Tristram-Nagle, J.F. Nagle, Structure of fully hydrated fluid phase DMPC and DLPC lipid bilayers using X-ray scattering from oriented multilamellar arrays and from unilamellar vesicles, Biophysical Journal 88 (2005) 2626–2637.
[8] J.K. Seydel, M. Wiese, Drug-Membrane Interaction: Analysis, Drug Distribution, Modeling, Wiley-VCH, 2002.
[9] M.P. Sheetz, S.J. Singer, Biological membranes as bilayer couples. A molecular mechanism of drug–erythrocyte interactions, Proceedings of the National Academy of Sciences of the United States of America 71 (1974) 4457–4461.
[10] L. Koubi, M. Tarek, M.L. Klein, D. Scharf, Distribution of halothane in a dipalmitoylphosphatidylcholine bilayer from molecular dynamics calculations, Biophysical Journal 78 (2000) 800–811.
[11] E. Okamura, Structure and dynamics of drugs in lipid bilayer membranes: an NMR application to drug delivery study, Membrane 28 (2003) 10.
[12] J.K. Seydel, E.A. Coats, H.P. Cordes, M. Wiese, Drug membrane interaction and the importance for drug transport, distribution, accumulation, efficacy and resistance, Archiv der Pharmazie (Weinheim) 327 (1994) 601–610.
[13] A. Berquand, M.P. Mingeot-Leclercq, Y.F. Dufrene, Real-time imaging of drug–membrane interactions by atomic force microscopy, Biochimica et Biophysica Acta 1664 (2004) 198–205.
[14] G.S. Lorite, T.M. Nobre, M.E. Zaniquelli, E. de Paula, M.A. Cotta, Dibucaine effects on structural and elastic properties of lipid bilayers, Biophysical Chemistry 139 (2009) 75–83.
[15] L.F. Fraceto, M. Pinto Lde, L. Franzoni, A.A. Braga, A. Spisni, S. Schreier, E. de Paula, Spectroscopic evidence for a preferential location of lidocaine inside phospholipid bilayers, Biophysical Chemistry 99 (2002) 229–243.
[16] H. Braun, Local Anesthesia: its Scientific Basis and Practical Use, 1914.
[17] S.Y. Wang, C. Nau, G.K. Wang, Residues in Na(+) channel D3-S6 segment modulate both batrachotoxin and local anesthetic affinities, Biophysical Journal 79 (2000) 1379–1387.
[18] M.F. Sheets, D.A. Hanck, Molecular action of lidocaine on the voltage sensors of sodium channels, Journal of General Physiology 121 (2003) 163–175.
[19] C. Nau, G.K. Wang, Interactions of local anesthetics with voltage-gated Na+ channels, Journal of Membrane Biology 201 (2004) 1–8.

[20] G.M. Lipkind, H.A. Fozzard, Molecular modeling of local anesthetic drug binding by voltage-gated sodium channels, Molecular Pharmacology 68 (2005) 1611–1622.
[21] M.F. Sheets, D.A. Hanck, Outward stabilization of the S4 segments in domains III and IV enhances lidocaine block of sodium channels, The Journal of Physiology 582 (2007) 317–334.
[22] A. Seelig, P.R. Allegrini, J. Seelig, Partitioning of local anesthetics into membranes: surface charge effects monitored by the phospholipid head-group, Biochimica et Biophysica Acta 939 (1988) 267–276.
[23] T. Hata, H. Matsuki, S. Kaneshina, Effect of local anesthetics on the bilayer membrane of dipalmitoylphosphatidylcholine: interdigitation of lipid bilayer and vesicle-micelle transition, Biophysical Chemistry 87 (2000) 25–36.
[24] L.F. Fraceto, A. Spisni, S. Schreier, E. de Paula, Differential effects of uncharged aminoamide local anesthetics on phospholipid bilayers, as monitored by 1H-NMR measurements, Biophysical Chemistry 115 (2005) 11–18.
[25] C.J. Hogberg, A.P. Lyubartsev, Effect of local anesthetic lidocaine on electrostatic properties of a lipid bilayer, Biophysical Journal 94 (2008) 525–531.
[26] Y. Boulanger, S. Schreier, I.C. Smith, Molecular details of anesthetic–lipid interaction as seen by deuterium and phosphorus-31 nuclear magnetic resonance, Biochemistry 20 (1981) 6824–6830.
[27] I.C. Smith, M. Auger, H.C. Jarrell, Molecular details of anesthetic–lipid interaction, Annals of the New York Academy of Sciences 625 (1991) 668–684.
[28] E. de Paula, S. Schreier, H.C. Jarrell, L.F. Fraceto, Preferential location of lidocaine and etidocaine in lecithin bilayers as determined by EPR, fluorescence and 2H NMR, Biophysical Chemistry 132 (2008) 47–54.
[29] D.P. Bossev, Z. Yi, The effect of the unsaturated double bond on the bending elasticity of lipid membranes studied by neutron spin echo, QENS 2006 conference proceedings, 2007, p. 7.
[30] H. Seto, N.L. Yamada, M. Nagao, M. Hishida, T. Takeda, Bending modulus of lipid bilayers in a liquid-crystalline phase including an anomalous swelling regime estimated by neutron spin echo experiments, The European Physical Journal E, Soft Matter 26 (2008) 217–223.
[31] M. Nagao, Z. Yi, D.P. Bossev, Bending elasticity of saturated and monounsaturated phopholipid membranes studied by the neutron spin echo technique, Journal of Physics: Condensed Matter 21 (2009).
[32] N. Kucerka, J. Pencer, J.N. Sachs, J.F. Nagle, J. Katsaras, Curvature effect on the structure of phospholipid bilayers, Langmuir 23 (2007) 1292–1299.
[33] H. Chakraborty, M. Sarkar, Interaction of piroxicam and meloxicam with DMPG/DMPC mixed vesicles: anomalous partitioning behavior, Biophysical Chemistry 125 (2007) 306–313.
[34] T. Lazaridis, Effective energy function for proteins in lipid membranes, Proteins 52 (2003) 176–192.
[35] O.S. Andersen, R.E. Koeppe II, Bilayer thickness and membrane protein function: an energetic perspective, Annual Review of Biophysics and Biomolecular Structure 36 (2007) 107–130.
[36] H. Duwe, E. Sackmann, Bending elasticity and thermal excitations of lipid bilayer vesicles: Modulation by solutes, Physica A: Statistical and Theoretical Physics 163 (1990) 410–428.
[37] T. Takeda, Y. Kawabata, H. Seto, S.K. Ghosh, D. Okuhara, S. Komura, M. Nagao, A. Brulet, J. Teixeira, Neutron spin echo investigations of membrane undulations in complex fluids involving amphiphiles, Journal of Physics and Chemistry of Solids 60 (1999) 3.
[38] N.L. Yamada, H. Seto, T. Takeda, M. Nagao, Y. Kawabata, K. Inoue, SAXS, SANS and NSE studies on “unbound” in DPPC/water/Cacl2 system, Journal of Physics Society of Japan 74 (2005) 2853–2859.
[39] A.G. Zilman, R. Granek, Undulations and dynamic structure factor of membranes, Physical Review Letters 77 (1996) 4788–4791.
[40] A.G. Zilman, S.A. Safran, Thermodynamics and structure of self-assembled networks, Physical Review E, Statistical, Nonlinear, and Soft Matter Physics 66 (2002) 051107.
[41] R. Nayar, M.J. Hope, P.R. Cullis, Generation of large unilamellar vesicles from long-chain saturated phosphatidylcholines by extrusion technique, Biochimica et Biophysica Acta 986 (1989) 200–206.
[42] C.J. Glinka, J.G. barker, B. Hammouda, S. Krueger, J.J. Moyer, The 30m small-angle neutron scattering instruments at the National Institute of Standards and Technology, Journal of Applied Crystallography 31 (1998) 430–445.
[43] C.J. Kline, Reduction and analysis of SANS and USANS data using IGOR Pro, Journal of Applied Crystallography 39 (2006) 6.
[44] B.D. Ladbrooke, D. Chapman, Thermal analysis of lipids, proteins and biological membranes. A review and summary of some recent studies, Chemistry and Physics of Lipids 3 (1969) 304–356.
[45] D. Chapman, The Structure of Lipids by Spectroscopic and X-ray Techniques, Methuen, Lodon, 1965.
[46] H. Yardimci, B. Chung, J.L. Harden, R.L. Leheny, Phase behavior and local dynamics of concentrated triblock copolymer micelles, Journal of Chemical Physics 123 (2005) 244908.
[47] M.C. Rheinstadter, W. Haussler, T. Salditt, Dispersion relation of lipid membrane shape fluctuations by neutron spin-echo spectrometry, Physical Review Letters 97 (2006) 048103.
[48] M. Monkenbusch, O. Holderer, H. Frielinghaus, D. Byelov, J. Allgaier, D. Richter, Bending moduli of microemulsions; comparison of results from small angle neutron scattering and neutron spin-echo spectroscopy, Journal of Physics: Condensed Matter 17 (2005) S2903.
[49] N. Rosov, S. Rathgeber, M. Monkenbusch, Neutron spin echo spectroscopy at the NIST Center for Neutron Research, Scattering from polymers-Characterization by X-rays, Neutrons, and Light, ACS symposium Series 739 (2000) 103–116.
[50] R.T. Azuah, L.R. Kneller, Y. Qiu, P.L.W. Tregenna-Piggott, C.M. Brown, J.R.D. Copley, R. M. Dimeo, DAVE: A comprehensive software suite for the reduction, visualization, and analysis of low energy neutron spectroscopic data, Journal of Research of the National Institute of Standard and Technology 114 (2009) 341–358.
[51] S. Mabrey, J.M. Sturtevant, Investigation of phase transitions of lipids and lipid mixtures by sensitivity differential scanning calorimetry, Proceedings of the National Academy of Sciences of the United States of America 73 (1976) 3862–3866.
[52] J. Stumpel, A. Nicksch, H. Eibl, Calorimetric studies on saturated mixed-chain lecithin-water systems. Nonequivalence of acyl chains in the thermotropic phase transition, Biochemistry 20 (1981) 662–665.
[53] T.P. McMullen, R.N. Lewis, R.N. McElhaney, Differential scanning calorimetric study of the effect of cholesterol on the thermotropic phase behavior of a homologous series of linear saturated phosphatidylcholines, Biochemistry 32 (1993) 516–522.
[54] E. Lissi, M.L. Bianconi, A.T. Doamaral, E. De Paula, L.E.B. Blanch, S. Schreier, Methods for the determination of partition-coefficients based on the effect of solutes upon membrane-structure, Biochimica et Biophysica Acta 1021 (1990) 46–50.
[55] E. de Paula, S. Schreier, Use of a novel method for determination of partition-coefficients to compare the effect of local-anesthetics on membrane-structure, Biochimica et Biophysica Acta-Biomembranes 1240 (1995) 25–33.
[56] M.A. Kiselev, E.V. Zemlyanaya, V.K. Aswal, R.H. Neubert, What can we learn about the lipid vesicle structure from the small-angle neutron scattering experiment? European Biophysics Journal 35 (2006) 477–493.
[57] J. Pencer, F.R. Hallett, Effects of vesicle size and shape on static and dynamic light scattering measurements, Langmuir 19 (2003) 7488–7497.
[58] J.B. Hayter, Physics of Amphiphiles: Micelles, Vesicles, and Microemulsions, North-Holland, Amsterdam, 1985.
[59] B.A. Lewis, D.M. Engelman, Lipid bilayer thickness varies linearly with acyl chain length in fluid phosphatidylcholine vesicles, Journal of Molecular Biology 166 (1983) 211–217.
[60] D. Uhrikova, G. Rapp, S. Yaradaikin, V. Gordeliy, P. Balgavy, Influence of local anesthetics on the phosphatidylcholine model membrane: small-angle synchrotron X-ray diffraction and neutron scattering study, Biophysical Chemistry 109 (2004) 361–373.
[61] S.T. Milner, S.A. Safran, Dynamic fluctuations of droplet microemulsions and vesicles, Physical Review A 36 (1987) 4371–4379.
[62] B. Farago, M. Monkenbusch, K.D. Goecking, D. Richter, J.S. Huang, Dynamics of microemulsions as seen by neutron spin-echo, Physica B-Condensed Matter 213 (1995) 712–717.
[63] J.H. Lee, S.M. Choi, C. Doe, A. Faraone, P.A. Pincus, S.R. Kline, Thermal fluctuation and elasticity of lipid vesicles interacting with pore-forming peptides, Physical Review Letters 105 (2010) 038101.
[64] M.C. Watson, F.L.H. Brown, Interpreting membrane scattering experiments at the mesoscale: the contribution of dissipation within the bilayer, Biophysical Journal 98 (2010) L9–L11.
[65] N. Kucerka, J. Pencer, M.P. Nieh, J. Katsaras, Influence of cholesterol on the bilayer properties of monounsaturated phosphatidylcholine unilamellar vesicles, The European Physical Journal E, Soft Matter 23 (2007) 247–254.
[66] J.H. Ren, S. Lew, Z.W. Wang, E. London, Transmembrane orientation of hydrophobic alpha-helices is regulated both by the relationship of helix length to bilayer thickness and by the cholesterol concentration, Biochemistry 36 (1997) 10213–10220.
[67] L. Coderch, J. Fonollosa, M. De Pera, J. Estelrich, A. De La Maza, J.L. Parra, Influence of cholesterol on liposome fluidity by EPR. Relationship with percutaneous absorption, Journal of Controlled Release 68 (2000) 85–95.
[68] W.W. Sulkowski, D. Pentak, K. Nowak, A. Sulkowska, The influence of temperature, cholesterol content and pH on liposome stability, Journal of Molecular Structure 744 (2005) 737–747.
[69] A.M. Smondyrev, M.L. Berkowitz, Structure of dipalmitoylphosphatidylcholine/cholesterol bilayer at low and high cholesterol concentrations: molecular dynamics simulation, Biophysical Journal 77 (1999) 2075–2089.
[70] P.L. Yeagle, Cholesterol and the cell-membrane, Biochimica et Biophysica Acta 822 (1985) 267–287.
[71] J. Gallova, D. Uhrikova, N. Kucerka, J. Teixeira, P. Balgavy, Hydrophobic thickness, lipid surface area and polar region hydration in monounsaturated diacylphosphatidylcholine bilayers: SANS study of effects of cholesterol and beta-sitosterol in unilamellar vesicles, Biochimica et Biophysica Acta-Biomembranes 1778 (2008) 2627–2632.
[72] I. Ueda, J.S. Chiou, P.R. Krishna, H. Kamaya, Local-anesthetics destabilize lipid membranes by breaking hydration shell: infrared and calorimetry studies, Biochimica et Biophysica Acta-Biomembranes 1190 (1994) 421–429.
[73] C.J. Hogberg, A. Maliniak, A.P. Lyubartsev, Dynamical and structural properties of charged and uncharged lidocaine in a lipid bilayer, Biophysical Chemistry 125 (2007) 416–424.
[74] L.L. Holte, K. Gawrisch, Determining ethanol distribution in phospholipid multilayers with MAS-NOESY spectra, Biochemistry 36 (1997) 4669–4674.
[75] Z.V. Leonenko, D.T. Cramb, Revisiting lipid — general anesthetic interactions (I): thinned domain formation in supported planar bilayers induced by halothane and ethanol, Canadian Journal of Chemistry 82 (2004) 1128–1138.
[76] D. Cramb, A. Carnini, H. Phillips, L. Shamrakov, Revisiting lipid — general anesthetic interactions (II): halothane location and changes in lipid bilayer microenvironment monitored by fluorescence, Canadian Journal of Chemistry 82 (2004) 1139–1149.
[77] K.C. Tu, M. Tarek, M.L. Klein, D. Scharf, Effects of anesthetics on the structure of a phospholipid bilayer: molecular dynamics investigation of halothane in the hydrated liquid crystal phase of dipalmitoylphosphatidylcholine, Biophysical Journal 75 (1998) 2123–2134.

[78] T.J. O'leary, P.D. Ross, I.W. Levin, Effects of anesthetic tetradecenols on phosphatidylcholine phase transitions. Implications for the mechanism of the bilayer pretransition, Biophysical Journal 50 (1986) 1053–1059.
[79] T. Heimburg, Mechanical aspects of membrane thermodynamics. Estimation of the mechanical properties of lipid membranes close to the chain melting transition from calorimetry, Biochimica et Biophysica Acta-Biomembranes 1415 (1998) 147–162.
[80] B. Pouligny, R. Dimova, C. Dietrich, Pretransitional effects in dimyristoylphosphatidylcholine vesicle membranes: optical dynamometry study, Biophysical Journal 79 (2000) 340–356.
[81] P. Meleard, C. Gerbeaud, T. Pott, L. FernandezPuente, I. Bivas, M.D. Mitov, J. Dufourcq, P. Bothorel, Bending elasticities of model membranes: influences of temperature and sterol content, Biophysical Journal 72 (1997) 2616–2629.
[82] E.A. Evans, Bending resistance and chemically-induced moments in membrane bilayers, Biophysical Journal 14 (1974) 923–931.
[83] E. Evans, W. Rawicz, K.C. Olbrich, T. McIntosh, D. Needham, Effect of chain length and unsaturation on elasticity of lipid bilayers, Biophysical Journal 79 (2000) 328–339.